

Importance of Thermal Disorder on the Properties of Alloys: Origin of Paramagnetism and Structural Anomalies in Iron-Aluminum

A. V. Smirnov and W. A. Shelton

Computer Science and Mathematical Division, Oak Ridge National Laboratory, Oak Ridge, TN 37831-6367

D. D. Johnson

Materials Science and Engineering and Frederick Seitz Materials Research Laboratory, University of Illinois, Urbana, IL 61801

(Dated: January 28, 2004)

The bcc-based $\text{Fe}_{1-x}\text{Al}_x$ exhibit interesting magnetic and anomalous structural properties as a function of composition and sample processing conditions arising from thermal or off-stoichiometric chemical disorder, and, although well studied, these properties are not understood. In stoichiometric B2 FeAl, including the effects of partial long-range order (i.e., thermal antisites), we find the observed paramagnetic response (with non-zero local moments), in contrast to past investigations which find ferromagnetism based on local density approximation (LDA) to density functional theory or which find a non-magnetic state from LDA+U, both of which are inconsistent with experiment. Moreover, from this magneto-chemical coupling, we are able to determine the origins of the lattice constant anomalies found in $\text{Fe}_{1-x}\text{Al}_x$ for $x \simeq 25 - 50$, as observed from various processing conditions.

Although bcc-based iron-aluminum ($\text{Fe}_{1-x}\text{Al}_x$) alloys have been investigated extensively over the years, the complex (even anomalous) structural and magnetic properties as a function of composition and state of chemical order are not well understood. In fact, while most experimental investigations observe Curie-Weiss-like paramagnetic (PM) responses with small ($\sim 0.3\mu_B$) effective moments on $\text{Fe}^{1,2,3,4}$, electronic-structure calculations for perfectly ordered B2 (β -CuZn) phase obtain a ferromagnetic (FM) state with $\mu \sim 0.7\mu_B^{4,5,6,7,8,9}$. In addition, experimentally in the iron-rich Fe-Al system, anomalies are observed in the average lattice constant that vary with processing conditions, i.e., whether the samples were quenched, annealed, and/or cold-worked¹⁰. The important fact is that the processing route used in preparing samples (stoichiometric or not) produces lattice defects that can have a significant effect on the mechanical, structural and magnetic properties of Fe-Al as well as on the intermetallics as a whole. Furthermore, there are competing structures: at 28% (38%) Al at 825 K (475 K), for example, the B2 phase undergoes a secondary-ordering transition to DO_3 (Fe_3Al or Heusler) phase. And, due to kinetic limitations, the phase diagram is known only for $T \geq 475$ K. To be able to compare to experiment and to gain an understanding of the anomalies found in this system will require a first principles method capable of including disorder and temperature effects on equal footing with the electronic structure.

Here, using first-principles methods, we investigate the structural and magnetic properties of bcc-based Fe-Al, including the A2 (bcc disordered), B2, and DO_3 phases, as a function of compositionally- and thermally-induced disorder (antisites). In B2 FeAl, we predict that the PM state competes with FM state when the state of partial long-range order is taken into account. In particular, at $T = 0$ K, the PM and FM states are degenerate in energy at $\sim 70\%$ of perfect long-range order but are near-degenerate (≤ 0.25 mRy/atom) over the range of 50 – 90% of order (partial order compatible with experiment); whereas FM state is ~ 0.5 mRy/atom lower than the PM (and nonmagnetic (NM)) state for perfectly ordered B2, in agreement with past theoretical work. More generally, this magneto-chemical coupling leads to anomalies in the average lattice constant in $\text{Fe}_{1-x}\text{Al}_x$ for $x \simeq 0.25 - 0.5$ at.%Al, reproducing what has been observed for annealed, quenched and cold-worked samples, but also never explained or found from theory. Our results provide a simple and physically reasonable understanding of the, heretofore, anomalous properties found in bcc-based Fe-Al.

I. DISCUSSION

Ordered intermetallics constitute an important class of high-temperature structural materials. One of the most common crystals structures in the intermetallics is the B2 structure, which because of its simple lattice structure makes it an ideal model for studying a variety of physical phenomena found in these systems¹¹. The physical properties of Fe-Al are quite sensitive to extrinsic defects^{12,13} and thermomechanical history^{10,14,15,16}. In fact, B2 FeAl is not fully ordered due to various lattice defects, such as vacancies and antisites, and they are thought to play a major role in the mechanical and magnetic behavior of this system. However, the precise concentration of the different lattice defects is not well known. Furthermore, unlike the strongly ordered intermetallics such as B2 NiAl, which forms triple defect structures consisting of two vacancies on the transition metal sublattice and an antisite defect on the Al sublattice, the possible defect structures for the less strongly ordered B2 FeAl are much more complicated, as the formation of both vacancies and antisite defects on the Fe site are thermodynamically stable¹⁷.

As mentioned, using the local density approximation (LDA) to density functional theory (DFT)¹⁸, electronic-structure calculations on ideal B2-FeAl obtain a FM state with $\mu \sim 0.7\mu_B$ ^{4,5,6,7,9}, in contradiction to the Curie-Weiss-like PM response found in experiment. Calculations based on the so-called disordered local moment (DLM) paramagnetic state have also been suggested, but this approach by itself was unable to explain experiment⁸. Calculations using generalized gradient approximation (GGA) to DFT, which are known to improve the magnetic ground-state description of elemental bcc Fe,¹⁹ have been employed but do not yield FM DO₃-Fe₃Al or NM B2-FeAl as a ground-state²⁰. On the other hand, recent investigations^{21,22} have obtained a NM ground-state for ideal B2 FeAl within so-called LDA+U procedure, which is an extension of LDA that introduces correlation corrections due to the orbital dependence of the Coulomb interaction. The LDA+U finds a NM ground-state for B2-FeAl for a particular range of the empirically chosen parameter U. However, once again, it is in contradiction to experiment, and does not confirm the LDA+U picture. Furthermore, none of these investigations address any other experimental observation, such as, the important composition-dependent structural anomalies strongly affected by processing.

In alloys, both short-range order and partial long-range order (LRO), and associated magnetism, are strongly affected by the processing temperatures, whether its an anneal or quench, which freezes in chemical disorder at that temperature (e.g. $0 < T_{Curie} < T_{processing} < T_{order-disorder}$). For example, DO₃-Fe₃Al crystal structure has $\sim 8\%$ site disorder according to Bradley and Jay²³, which was as later confirmed^{24,25}. Thus, the overall processing procedure affects greatly the materials properties and, therefore, the characterization data obtained from samples that are not completely ordered (due to kinetic limitations). The aforementioned DFT calculations provide results for perfectly ordered states or off-stoichiometric disorder corresponding to T=0 K, which may not be directly related to the experimentally assessed data. However, Johnson et. al.²⁶ have shown that including the thermally-induced partial LRO effects allows quantitative comparisons to characterization experiments, and explains discrepancy of $T = 0$ K DFT results. Clearly an investigation of the effects of (thermally-induced or off-stoichiometry) partial order on the magnetic and structural properties in the B2 FeAl system is in order.

II. COMPUTATIONAL DETAILS

For our electronic-structure calculations, we use the Green's function based, multiple-scattering approach of Korringa, Kohn and Rostoker (KKR)^{27,28}. We use the local density approximation to the exchange-correlation potential and energy as parameterized by Von-Barth-Hedin²⁹. In addition, all calculations are performed using the atomic sphere approximation (ASA) with equal size Fe and Al atomic spheres³⁰.

By using the KKR method, we can include chemical and magnetic disorder in the electronic structure and energetics via the coherent potential approximation^{31,32} (CPA) modified to incorporate improved metallic screening due to charge-correlations arising from the local chemical environment³³. The KKR-CPA density-functional theory and total energy formalism provides reliable and well-documented energetics and structural-related parameters, from fully disordered to ordered configurations.

We describe the PM state by the disorder local moment (DLM) approximation^{34,35,36}, where magnetic short-range order is ignored, yet the site-dependent average effect of magnetic orientational disorder is self-consistently included, whether chemically ordered (partially or fully) or disordered. Thus, our implementation of the KKR-CPA is capable of treating simultaneously chemical disorder, site defects and magnetic (orientational) disorder all on equal footing with the electronic structure (e.g., Slater-Pauling curve³⁷, or the INVAR^{38,39}).

For all calculations we use a four-atoms unit cell (see Fig. 1) based on an underlying bcc crystal lattice that inherently contains the DO₃, B2 and A2 (bcc disordered) structures as a function of long-range order or composition because each sublattice is composed locally of Fe_{1-x}Al_x. Using Fig. 1 it is easy to define order parameters needed. For example, referenced to the Al sublattice ($i = \text{Al}$), the B2 ordering at $x=1/2$ can be defined in terms of a temperature-dependent LRO parameter $\eta(T)$: $c_{i=\text{Al}}^{\text{Al}} = \frac{1}{2}(1 + \eta(T))$ and $c_{i=\text{Al}}^{\text{Fe}} = \frac{1}{2}(1 - \eta(T))$, giving the fully disordered A2 (ordered B2) lattice for $\eta=0$ (1). This describes a static compositional modulation of the A2 phase by a wavevector $\mathbf{k}_0=2\pi(1,1,1)/a$ to yield the partially-ordered B2 FeAl ("pseudo-FeAl"), see, e.g., Ref. 40.

Characterization is performed on samples at finite temperatures with $0 < \eta(T) < 1$. The temperature dependence of $\eta(T)$ can only be obtained from a thermodynamic calculation or measurement. In Fe-Al, $\eta(T)$ varies continuously in the solid phase (for DO₃ with arbitrary x, it can be done via two LRO parameters for the two operative wavevectors, i.e, (111) and $(\frac{1}{2}\frac{1}{2}\frac{1}{2})$ ⁴⁰). Hence, a Landau expansion of the free energy difference in terms of $F(\eta)$ (relative to $\eta=0$ state) for a given fixed-sized unit cell, DO₃-type in our case, is written as

$$\begin{aligned} \Delta F^\sigma(\eta) &= F^{(2),\sigma}(0)\eta^2 + O(\eta^4) \\ &= E^\sigma(\eta) - E^\sigma(0) - T\Delta S(\eta), \end{aligned} \quad (1)$$

where odd powers of η are zero due to the translational symmetry of the A2 ($\eta = 0$) phase, and ΔS is an entropy difference for the magnetic state $\sigma = (\text{DLM}, \text{FM}, \text{or NM})$. We note that the largest contribution to the entropy is the point

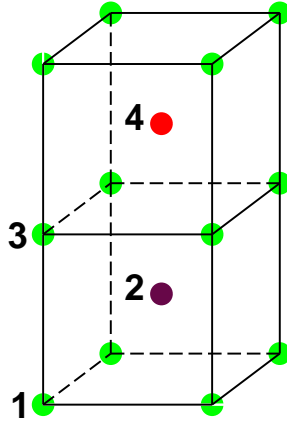


Figure 1: The four-atom cell used to study cubic DO_3 . For basis atoms 1-4, the translational vectors in lattice units of $\mathbf{T}_1=(101)$, $\mathbf{T}_2=(011)$, $\mathbf{T}_3=(001)$ generate the standard 16-atom (cubic) DO_3 cell. In ideal DO_3 Fe_3Al , Fe (Al) occupies sites 1-3 (site 4); whereas in B2 FeAl , Fe (Al) atoms occupy odd (even) numbered site. Sites 1 and 3 are always equivalent.

entropy and this cancels exactly within a common unit cell; also, when the nearest-neighbor (chemical) environments are approximately the same (as roughly is the case here), the nearest-neighbor pair entropy cancels exactly. Therefore, the temperature effects are primarily due to antisite disorder, and (for fixed composition) can be accounted for by analyzing total energy differences. (See Ref. 26 for how such calculations are related to characterization experiments.)

In addition to calculations of B2 FeAl versus η , fully ordered FeAl and Fe_3Al , we also consider $\text{Fe}_{1-x}\text{Al}_x$ with Al concentration between 25% and 50%: fully-disordered and off-stoichiometric-disordered B2 and DO_3 with and without chemical disorder on the Al sublattices (marked 2 and 4 in Fig. 1). Specifically, the following cases of constituent concentrations are investigated:

- (i) For $0.25 \leq x \leq 0.50$: $c_1^{\text{Al}} = c_3^{\text{Al}} = 0$, $c_4^{\text{Al}} = 1$, $c_2^{\text{Al}} = 4x - 1$;
- (ii) For $0.25 \leq x \leq 0.50$: $c_1^{\text{Al}} = c_3^{\text{Al}} = 0$, $c_2^{\text{Al}} = c_4^{\text{Al}} = 2x$;
- (iii) For $0.25 \leq x \leq 0.25 + x_0/2$: $c_4^{\text{Al}} = 1 - x_0$, $c_1^{\text{Al}} = c_2^{\text{Al}} = c_3^{\text{Al}} = (4x - (1 - x_0))/3$;
- (iv) For $0.25 + x_0/2 \leq x \leq 0.40$: $c_4^{\text{Al}} = 1 - x_0$, $c_1^{\text{Al}} = c_3^{\text{Al}} = x_0$, $c_2^{\text{Al}} = (4x - 1 - x_0)$;
- (v) For $0.25 \leq x \leq 0.25 + x_0/2$: $c_1^{\text{Al}} = c_3^{\text{Al}} = (4x - (1 - x_0))/3$, $c_2^{\text{Al}} = c_4^{\text{Al}} = 0.5 - x_0/3$;
- (vi) For $0.25 + x_0/2 \leq x \leq 0.50$: $c_1^{\text{Al}} = c_3^{\text{Al}} = x_0$, $c_2^{\text{Al}} = c_4^{\text{Al}} = 2x - x_0$.

Cases (i) and (ii) have no disorder on sublattices 1 and 3 and *ideal* (no LRO) DO_3 and B2 compositions for off-stoichiometric $\text{Fe}_{1-x}\text{Al}_x$, (iii)-(vi) are used to simulate possible compositions with LRO, i.e. thermodynamic chemical disorder. Concentrations of the constituents for sublattices 1 and 3 are assumed to be the same both in DO_3 and B2, and the Al content is not more than x_0 (see Fig. 1 caption). The value of $x_0=0.09$ is chosen somewhat arbitrarily for illustrative purpose, although it is comparable with the disorder reported experimentally from DO_3 -type Fe-Al in Ref.²³; for B2 FeAl it corresponds $\eta = 1 - 2x_0 = 0.82$.

III. PARAMAGNETISM IN B2 FEAL

As mentioned, experimentally B2 FeAl is found to be paramagnetic, with finite local moments. Yet, in agreement with previous theoretical work^{4,5,6,7,9} our calculations find that the *ideal* B2 FeAl is ferromagnetic. At the theoretical equilibrium lattice parameter $a = 5.34$ Bohr, we obtain a magnetic moment of $\approx 0.72\mu_B$ for Fe and $-0.03\mu_B$ for Al, again consistent with the published data. However, such calculations ignore the fact that B2 FeAl is not fully ordered at any finite temperature.

Therefore, in Fig. 2, we show the stability of FM, NM and DLM partially ordered phases of FeAl alloy versus long-range order, η , relative to that of the fully-disordered FM state.

The NM-FM energy difference decreases monotonically as $\eta \rightarrow 1$ (increasing order) from 4.8 mRy/atom in the A2 state to 0.5 mRy/atom in the fully ordered B2 structure. For $\eta = 0$ (A2) the DLM-FM energy difference, $\Delta E^{\text{DLM-FM}}$, is ~ 3.8 mRy/atom ($a^{\text{FM}} = 5.45$ Bohr) with $\mu_{\text{Fe}}^{\text{FM}} = 1.83\mu_B$ and $\mu_{\text{Fe}}^{\text{DLM}} = 1.32\mu_B$, respectively. We find that the FM state is nominally always the lowest energy state for any value of η ($\Delta E^{\text{DLM-FM}} \leq 0.25$ mRy/atom, i.e., less than thermal energies, for $0.9 \geq \eta \geq 0.5$), except at $\eta \sim 0.7$ ($1 - \eta^2 = 0.5$) where the FM state is degenerate with the DLM state. For this nearly ordered B2 structure, $\eta = 0.7$ corresponds to a 15% concentration of Al on the Fe rich sublattice, compatible with $\sim 19\%$ from experiment^{4,10}. Both the FM and DLM states have nearly the same

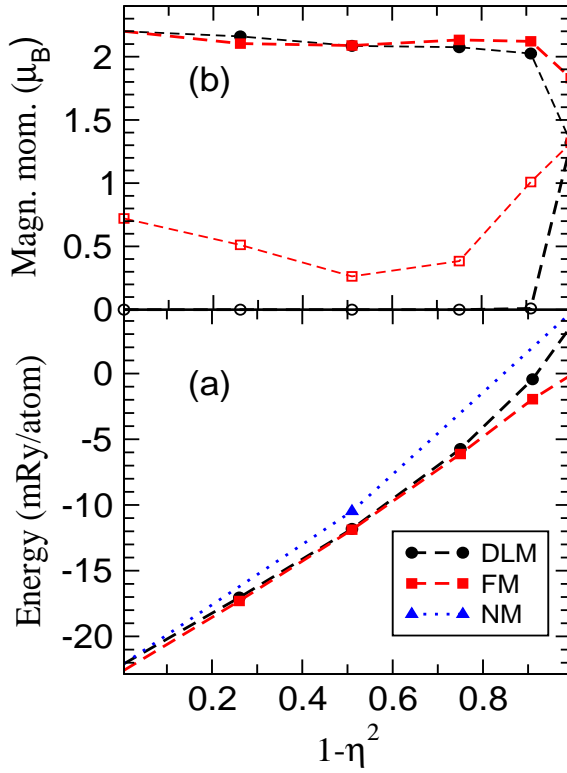


Figure 2: The DLM (circles), FM (squares) and NM (triangles) (a) total energies relative to the A2 FM (mRy/atom) and (b) Fe magnetic moments (μ_B) versus partial order $1 - \eta^2$, with filled symbols the Al-rich sites (i.e., the Fe anti-sites).

lattice parameter (5.36 Bohr). The local Fe anti-sites moments are finite for any partial long-range order, see Figure 2. Whereas Fe atoms on Al-rich sites have nearly the same magnetic moments ($\sim 2.1\mu_B$) for both FM and DLM states, the Fe moments for the other sites only exist in the FM state where they are relatively small. The average PM local moments are comparable to the observed Curie-Weiss moments $\sim 0.3\mu_B$ at $\eta = 0.7$.

It is clear that antisite defects play a crucial role in determining the magnetic configuration. However, in the DLM state at $\eta < 0.3$ (see Fig. 2b), the Fe magnetic moments exist in both high- and low-spin states, similar to bcc Fe; while in the fully-ordered B2-phase ($\eta = 1$), the DLM state is equivalent to the NM state, where all local moments are equal to zero (quenched). As an aside, we note that the PM state (stabilized, as identified here, by the antisite disorder) may benefit from further stabilization afforded by the LDA+U procedure^{21,22}, but it is not the origin for the PM effect, as is now clear.

The key point is that the FM and DLM states can be degenerate or nearly degenerate in the partially ordered equiatomic FeAl state. Furthermore, Monte Carlo simulations⁴¹ of A2 FeAl (i.e. $\eta = 0$) also obtain a paramagnetic state at room temperature. The important quantity in understanding non-zero temperature phenomena is the free energy and the disordered B2-DLM magnetic phase has a larger configurational entropy contribution to the free energy than the B2-FM ordered structure over a wide range of η . Thus, partial long range chemical order is stable, making the paramagnetic DLM state the stable configuration at finite temperature, even with only a small degree of disorder.

We note that the theoretical DLM lattice constant is about 3% below the experimental value (≈ 5.50 Bohr). However, such a deviation is comparable with pure bcc-Fe, as found in other calculations. The calculated DLM magnetic moment on an antisite Fe atom (i.e. on Al-rich sites) is close to the value of $2.2\mu_B$ observed by Parthasarathi and Beck² for samples quenched in cold water. In addition, Bogner *et al.*⁴ have extracted a moment of $\approx 3.43\mu_B$ from Langevin-type behavior of magnetization-field dependence. Bogner *et al.* hypothesized that such a moment could result from a cluster formed by nine nearest Fe atoms, which would correspond to a partially-ordered alloy with a concentration of Fe atoms on Al sites of $\sim 18\%$, close to the 19.12% found in experiment. Again, it is similar to the disorder we find needed for degeneracy in our calculations, i.e., $\sim 15\%$ with $\eta = 1 - 2(0.15) = 0.7$.

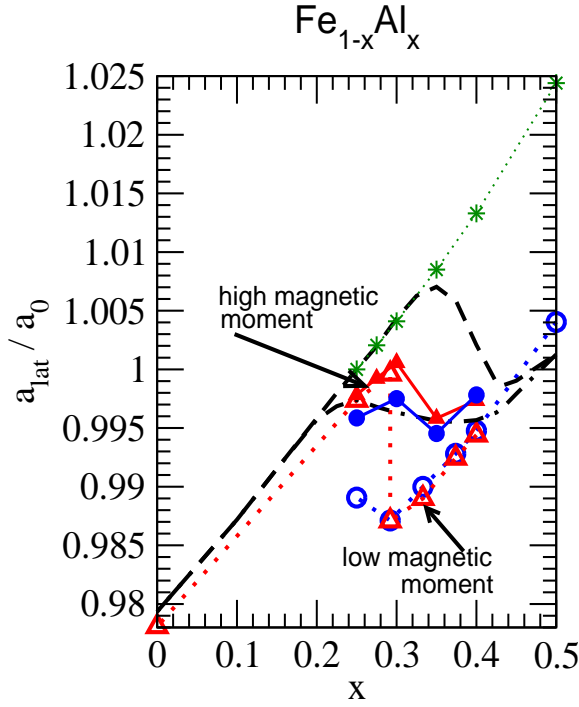


Figure 3: Reduced lattice parameter of $\text{Fe}_{1-x}\text{Al}_x$ versus x . Theory results are for *off-stoichiometric* DO_3 (triangles) and B2 (circles), or the A2 phases (stars). Theoretical $a_0(5.320 \text{ Bohr})$ is the lattice constant of the A2 at $x=0.25$. Filled symbols (triangles/circles) are for $\text{DO}_3/\text{B2}$ with additional thermal (antisite) disorder, see text. Experimental data is the dashed (dash-dotted) line for as-deformed samples (quenched from 1273 K)¹⁰, and a_0 is that observed lattice constant at $x=0.25$ for deformed sample. Quenching from 523 K yields similar results to high-T quench data.

IV. STRUCTURAL ANOMALIES IN FE-RICH FE-AL

Lattice constant anomalies have been experimentally observed in the Fe-rich region of the Fe-Al phase diagram. The lattice constant dependence on concentration is strongly dependent on the quenching or annealing procedure¹⁰ used in synthesizing the material (dashed line in Fig. 3), i.e. thermal antisites and vacancies. For low Al concentration the lattice constant has a nearly linear dependence on concentration. However, between 25%-40% the lattice parameter exhibits non-monotonic behavior with a maximum lattice constant at $x < 0.3$ (for deformed samples at $x \sim 0.34$) and a minimum between $0.34 < x < 0.43$ with increasing Al content. Of course, the exact behavior strongly depends on the type of quenching procedure used during processing¹⁰. On the other hand, the experimental data do not provide quantitative information on (chemical and magnetic) sample-dependent disorder in the observed²³ partially ordered DO_3 and B2 structures, which have chemical disorder on each independent sublattice (estimated to about 8% near $x = 0.25$) and partial long-range order. It is assumed that the formation of the "pseudo-FeAl" type of ordering is associated with the structural anomalies¹⁰.

First, to address the anomalies, we consider the "ideal" DO_3 : case (i) – with disorder only on the Al sublattice 4; and ideal B2: case (ii) – with disorder on the Al sublattices 2 and 4.

Our DO_3 calculations exhibit linear growth of the lattice constant with increasing concentration up to $x \sim 0.29$, while the average magnetic moment (per atom) μ decreases from $1.42\mu_B$ at $x = 0.25$ to $1.23\mu_B$. At $x \simeq 0.29$ two degenerate solutions exist for the FM state. The *low-spin* solution has both a smaller $\mu \sim 0.54\mu_B$ and a smaller lattice constant (see Fig. 3). However, the largest discrepancy is for the Fe magnetic moments on sites 1 and 3 where the *low-spin* solution has a significantly smaller magnetic moment on these sites ($\sim 0.2\mu_B$) as compared to *high-spin* solution ($\sim 1.52\mu_B$) on the same sites. Above $x=0.29$, the *low-spin* solution is energetically more favorable; at elevated temperatures a smooth transition from one solution to the second solution should be expected due to the possible coexistence of both solutions in a range of Al concentration.

In addition we note that the calculated lattice parameter of the fully-disordered A2 phase is almost linear for concentrations of Al up to 34% which agrees well with experimental observations for deformed samples quenched at high temperatures, see Fig. 3. For the A2 phase the energy is about 7 mRy larger than "ideal" DO_3 at $x = 0.25$, see Fig. 4. The respective energy difference begins to grow rapidly with increasing Al concentration at $x \sim 0.3$: from 8.4

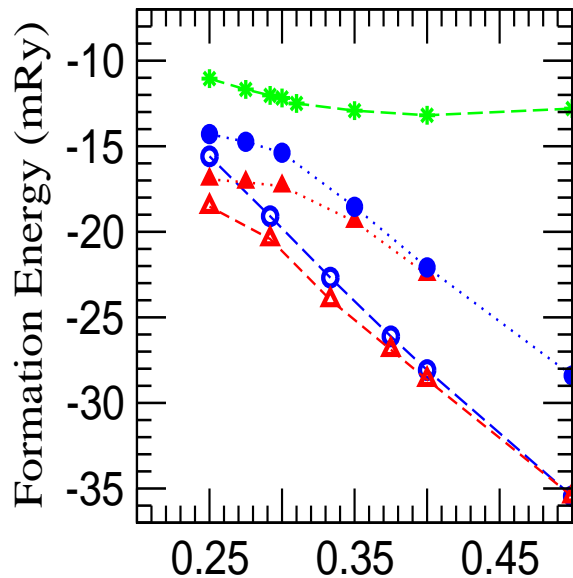


Figure 4: Formation energy of ferromagnetic A2, DO₃ and B2 Fe_{1-x}Al_x versus concentration of Al; symbols are chosen as in Fig. 3.

mRy at $x = 0.29$ to 22.6 mRy at $x = 0.5$.

Consideration of the "ideal" B2-disordered Fe_{1-x}Al_x reveals that the lattice parameter is practically indistinguishable from the *low-spin* solution in DO₃ calculations, however, with magnetic moments that are slightly higher than the ones found in DO₃. The difference in the total energy between *pseudo*-FeAl and "ideal" DO₃ declines rapidly, see Fig. 4, from 2.9 mRy/atom at $x=0.25$ to 0.5 mRy/atom at $x=0.40$ and finally to zero at $x=0.5$, where the chemical structures are equivalent. Taking into account that *pseudo*-FeAl configurational entropy contribution to free energy is larger than in partially-ordered DO₃ for the same composition, it is reasonable to expect that at finite temperature off-stoichiometric DO₃ and B2 phases could coexist for some values of x . For high enough Al content DO₃ would eventually be replaced by the B2 phase as the ground state where again the actual value for the Al concentration would depend on both the temperature and processing procedure.

To illustrate the importance of the thermodynamical chemical disorder we performed calculations for both DO₃ (iii,iv) and B2 (v,vi) phases. Figure 3 shows a stronger lattice constant dependence on concentration for B2 than for the "high-spin" DO₃ solution (i.e. at $x < 0.3$). For larger Al content the influence on B2 and DO₃ is comparable. In addition, the linear dependence of the formation energy on the Al concentration is virtually unaffected by the chemical disorder (excluding the uniform shift), see Fig. 4, for $x > 0.34$. However, for smaller Al concentrations this is not the case. This is due to the dependence of the sublattice composition on Al content in (iii)-(vi). The additional effect of partial-order on top of off-stoichiometric disorder leads roughly to a plateau in the formation energy, especially for DO₃ (see Fig. 4), which is compatible with the shift off stoichiometry for the maximum in the B2-DO₃ transition temperature.

Generally, the magneto-chemical coupling effect is a ubiquitous phenomena observed in many materials. It has been used also to explain quantitatively, e.g., ordering characterization data²⁶ and INVAR lattice anomaly in Fe-Ni⁴².

V. SUMMARY

The structural and magnetic anomalies observed in bcc-based Fe-Al have remained unexplained experimentally and theoretically for over 50 years. As characterization data and their interpretation depend upon the sample preparation and processing, the analysis of their properties based on simulation require the inclusion of these important thermal effects. We presented a theoretical study that incorporates magnetic, off-stoichiometric and thermodynamic chemical disorder on equal footing with the electronic structure, exemplifying a quantitative means for studying materials processed at high temperatures where point defects (such as anti-sites) play an important role in determining the properties. We find that partial long-range order due to thermal (i.e. antisite) disorder yields paramagnetic B2 FeAl (with finite moments) that is stable with respect to the ferromagnetic state, in contrast to past theory but in agreement with experiment. The partial order required also agrees with experiment. In addition, we showed

that this same magneto-chemical coupling produces structural anomalies observed versus Al content. Our results provide a clear and simple explanation behind the observed paramagnetism and structural anomalies in Fe-Al. We expect that this type of long-range order effect is responsible for the observed Fe₃Al lattice constant dependence on annealing temperature⁴³, as well as the paramagnetism (or spin-glass behavior⁴⁴) in B2-Fe_{1-x}Al_x, both of which may be investigated using the approach employed here for Fe_{0.5}Al_{0.5}.

Acknowledgments

This research is supported by the Mathematical, Information and Computational Sciences, Office of Advanced Scientific Computing Research, U.S. Department of Energy at Oak Ridge National Laboratory under Contract DE-AC05-00OR22725 with UT-Battelle Limited Liability Corporation, and at the Frederick Seitz Materials Research Laboratory under contract DEFG02-91ER45439.

-
- ¹ M. J. Besnus, A. Herr, and A. J. P. Meyer, *J. of Phys. F* **5**, 2138 (1975).
² A. Parthasarathi and P. A. Beck, *Solid State Commun.* **18**, 211 (1976).
³ H. Domke and L. K. Thomas, *J. of Magn. Magn. Mater.* **45**, 305 (1984).
⁴ J. Bogner, W. Steiner, M. Reissner, P. Mohn, P. Blaha, K. Schwarz, R. Krachler, H. Ipser, and B. Sepiol, *Phys. Rev. B* **58**, 14922 (1998).
⁵ A. R. Williams, J. Kübler, and J. C. D. Gellat, *Phys. Rev. B* **19**, 6094 (1979).
⁶ H. Chacham, E. G. da Silva, D. Guenzburger, and D. E. Ellis, *Phys. Rev. B* **35**, 1602 (1987).
⁷ V. Sundararajan, B. R. Sahu, D. G. Kanhere, P. V. Panat, and G. P. Das, *J. of Phys.: Condens. Matter* **7**, 6019 (1995).
⁸ S. K. Bose, V. Drchal, J. Kudrnovsky, O. Jepsen, and O. K. Andersen, *Phys. Rev. B* **55**, 8184 (1997).
⁹ N. I. Kulikov, A. V. Postnikov, G. Borstel, and J. Braun, *Phys. Rev. B* **59**, 6824 (1999).
¹⁰ W. Hume-Rothery, R. E. Smallman, and C. W. Haworth, *The Structure of Metals and Alloys* (The Metals and Metallurgy Trust of the Institute of Metals and Institution of Metallurgists, London, 1969), pp. 172–173.
¹¹ I. Baker and P. R. Munroe, in *High Temperature Aluminides and Intermetallics*, edited by S. H. Whang, C. Liu, D. Pope, and J. Stiegler (The Minerals, Metals and Material Society, 1990), pp. 425–452.
¹² C. T. Liu, E. H. Lee, and C. G. Mckamey, *Scr. Metall.* **23**, 875 (1989).
¹³ S. Takahashi and Y. Umakoshi, *J. Phys.: Condens. Matter* **3**, 5805 (1991).
¹⁴ P. Nagpal and I. Baker, *Metall. Trans.* **21A**, 2281 (1990).
¹⁵ Y. A. Chang, L. M. Pike, C. T. Liu, A. R. Billbrey, and D. S. Stone, *J. Intermetall.* **1**, 107 (1993).
¹⁶ D. Weber, M. Meurtin, D. Paris, A. Fourdeux, and P. Lesbats, *J. Phys. C* **7**, 332 (1997).
¹⁷ C. L. Fu, Y. Y. Ye, M. H. Yoo, and K. M. Ho, *Phys. Rev. B* **48**, 6712 (1993).
¹⁸ S. Lundqvist and N. H. March, eds., *Theory of the Inhomogeneous Gas* (Plenum, New York, 1983).
¹⁹ C. Elsässer, J. Zhu, S. G. Louie, M. Fähnle, and C. T. Chan, *J. Phys.: Condens. Matter* **10**, 5081 (1998).
²⁰ F. Lechermann, F. Welsch, C. Elsässer, C. Ederer, and M. Fähnle, *Phys. Rev. B* **65**, 132104 (2002).
²¹ P. Mohn, C. Persson, P. Blaha, K. Schwarz, P. Novak, and H. Eschrig, *Phys. Rev. Lett.* **87**, 196401 (2001).
²² A. G. Petukhov, I. I. Mazin, L. Chioncel, and A. I. Lichtenstein, *Phys. Rev. B* **67**, 153106 (2003).
²³ A. J. Bradley and A. H. Jay, *Proc. R. Soc. London* **136**, 210 (1932).
²⁴ A. Taylor and R. M. Jones, *Phys. Chem. Solids* **6**, 16 (1958).
²⁵ A. Lawley and R. W. Cahn, *Phys. Chem. Solids* **20**, 204 (1961).
²⁶ D. D. Johnson, A. V. Smirnov, J. B. Staunton, F. J. Pinski, and W. A. Shelton, *Phys. Rev. B* **62**, R11917 (2000).
²⁷ J. Koringa, *Physica* **13**, 392 (1947).
²⁸ W. Kohn and N. Rostoker, *Phys. Rev.* **94**, 1111 (1954).
²⁹ U. von Barth and L. Hedin, *J. Phys. C* **5**, 1629 (1972).
³⁰ All angular momentum expansions include up to $l_{max}=3$; a semi-circular contour in complex plane with 18 points is used to integrate the Green's function over energy; at each energy, a Brillouin zone integration is performed by a special k-points method with 144 k-points. Such choices provides better than 0.1mRy/atom relative accuracy in total energy.
³¹ D. D. Johnson, D. M. Nicholson, F. J. Pinski, B. L. Györfy, and G. M. Stocks, *Phys. Rev. Lett.* **56**, 2088 (1986).
³² D. D. Johnson, D. M. Nicholson, F. J. Pinski, B. L. Györfy, and G. M. Stocks, *Phys. Rev. B* **41**, 9701 (1990).
³³ D. D. Johnson and F. J. Pinski, *Phys. Rev. B* **48**, 11553 (1993).
³⁴ J. Hubbard, *Phys. Rev. Lett.* **51**, 300 (1983).
³⁵ H. Hasagawa, *J. Phys. Soc. Jpn.* **46**, 1504 (1979).
³⁶ J. B. Staunton, B. Györfy, A. J. Pindor, G. M. Stocks, and H. Winter, *J. Phys. F: Met. Phys.* **15**, 1387 (1985).
³⁷ D. D. Johnson, F. J. Pinski, and J. B. Staunton, *J. Appl. Phys.* **61**, 3715 (1987).
³⁸ D. D. Johnson, F. J. Pinski, J. B. Staunton, B. L. Györfy, and G. M. Stocks, in *Physical Metallurgy of Controlled Expansion "INVAR-type" Alloys*, edited by K. Russell and D. Smith (Minerals, Metals, Materials Society, Materials Park, OH, 1989), pp. 3–24.

- ³⁹ D. D. Johnson and W. A. Shelton, in *The INVAR Effect - A Centennial Symposium*, edited by J. Wittenauer (Minerals, Metals, Materials Society, Materials Park, OH, 1997), p. 6374.
- ⁴⁰ A. G. Khachaturyan, *Theory of Structural Phase Transformations in Solids* (Wiley, New York, 1983), pp. 45–46.
- ⁴¹ J. Restrepo, G. A. P. Alcázar, and D. P. Landau, *J. Appl. Phys.* **89**, 7341 (2001).
- ⁴² V. Crisan, P. Entel, H. Ebert, H. Akai, D. D. Johnson, and J. B. Staunton, *Phys. Rev. B* **66**, 014416 (2002).
- ⁴³ Y. P. Selisskiy, *Fiz. Metal. i Metalloved.* **4**, 191 (1957).
- ⁴⁴ P. Shukla and M. Wortis, *Phys. Rev. B* **21**, 159 (1980).